Journal of Applied Pharmaceutical Research
Volume 13 Issue 2, Year of Publication 2025, Page 127 – 138
DOI: https://doi.org/10.69857/joapr.v13i2.1008

Check for updates

Research Article

JOURNAL OF APPLIED PHARMACEUTICAL RESEARCH | JOAPR
www.japtronline.com ***ISSN: 2348 – 0335***

EXPLORING 1,3,4-OXADIAZOLE DERIVATIVES FOR HEPATOCELLULAR CARCINOMA: SYNTHESIS, AND BIOACTIVITY EVALUATION

Mohini Patidar[1,2]*, Raghvendra Dubey[1], Nitin Deshmukh[3]

Article Information
Received: 10th January 2025
Revised: 29th March 2025
Accepted: 15th April 2025
Published: 30th April 2025

Keywords
1,3,4-oxadiazole, Hepatocellular carcinoma, Tyrosine kinase inhibitor, EGFR, In-vitro study.

ABSTRACT

Background: Cancer is a leading cause of death globally, with existing treatments often limited by resistance and toxicity. This necessitates the development of new, more effective anticancer therapies. **Methodology:** This study used *In-silico* modeling with tools like Pre-ADMET and Molinspiration to evaluate the physicochemical, pharmacokinetic, and pharmacodynamic properties of substituted 1,3,4-Oxadiazole derivatives. **Results and discussion:** Computational studies of 1,3,4-Oxadiazole analogues showed promising drug-like properties and bioavailability. To test the inhibitory efficacy against the protein target tyrosine kinase (PDB: 1M17), 30 designed derivative compounds underwent molecular docking experiments. 10 synthesized derivatives were structurally confirmed through Mass**,** NMR**,** and IR spectrometry, ensuring their purity and identity. Molecular docking and in vitro tests identified compound S23 as a potent tyrosine kinase inhibitor, with significant anti-proliferative activity (GI50: 0.25665634) and enzyme inhibition (IC50: 1.87), highlighting its potential as a therapeutic agent. **Conclusion:** According to our findings, the substituted derivative might offer superior potential for developing anticancer medicine.

INTRODUCTION

HCC is the most common type of liver cancer, frequently arising in the context of chronic liver diseases such as hepatitis B, alcoholic and fatty liver cirrhosis, contributing to significant morbidity and mortality [1]. The FDA has approved many anti-HCC drugs, such as Sorafenib (2007), Regorafenib (2017), Atezolizumab (2017), Lenvatinib (2018), and Bevacizumab (2020). These drugs share a focus on treating advanced liver cancer through targeted mechanisms, with overlapping goals of reducing angiogenesis and tumor growth [2]. However, their specific molecular targets, mechanisms of action, and potential side effect profiles differ, influencing their clinical use and efficacy. Cancer cells grow uncontrollably due to genetic mutations that disrupt normal regulatory mechanisms, leading to uncontrolled cell proliferation and the ability to resist therapeutic interventions. HCC cell develops drug resistance due to genetic mutations, activation of alternative survival pathways, overexpression of drug-efflux pumps, and changes in the tumor microenvironment, all of which reduce the effectiveness of therapies [3,4]. Although these drugs are effective, potential side

[1]*Department of Pharmaceutical Chemistry, Sage University, Institute of Pharmaceutical Sciences, Indore, MP 452016, India*
[2]*Department of Pharmaceutical Chemistry, GRY Institute of Pharmacy, Borawan, MP 451228, India*
[3]*Department of Pharmaceutical Chemistry, Mangaldeep Institute of Pharmacy, Aurangabad, Maharashtra 431001, India*

For Correspondence: **mohinipatidar321@gmail.com**

effects such as hypertension, fatigue, and proteinuria may occur. It's important to monitor for these adverse events during treatment. Additionally, the development of drug resistance can occur, potentially impacting treatment efficacy. Regular follow-up with healthcare providers is essential to manage these issues effectively [5]. The cost of anti-liver cancer medications is high due to factors such as complex drug development processes, limited patient population, high research and development costs, regulatory requirements, patent protection, and reduced competition. For example, the availability of generic versions of Sorafenib, like Sorafenat produced by NatcoPharma, helps mitigate some of these costs, making the treatment more affordable for patients despite the overall high cost structure [6]. These heterocyclic frameworks play a crucial role in anticancer research due to their structural versatility, enabling the design of second- or third-generation drugs with improved potency, selectivity, and pharmacokinetic properties. Their ability to target specific molecules such as kinases, topoisomerases, and DNA/RNA makes them valuable in overcoming drug resistance and off-target toxicity. Additionally, heterocyclic compounds can mimic or interfere with natural molecules like nucleotides, amino acids, and cofactors, facilitating the development of personalized cancer treatments, thus enhancing the potential for more effective and targeted therapies [7]. 1,3,4-Oxadiazole derivatives have emerged as a significant class of heterocyclic compounds due to their diverse pharmacological properties, including antimicrobial, anticancer, anti-inflammatory, anticonvulsant, and antiviral activities. Their unique five-membered ring structure, containing nitrogen and oxygen atoms, contributes to their stability and ability to interact with various biological targets. Importantly, the 1,3,4-Oxadiazole scaffold is often used as a bioisostere for esters, amides, and carbamates, enhancing drug-like properties such as metabolic stability and lipophilicity. Given these favorable characteristics, there is a growing interest in exploring novel 1,3,4-Oxadiazole derivatives as potential therapeutic agents [8].

EGFR kinase is a rational target in HCC due to its overexpression. It promotes cell proliferation, survival, and metastasis signaling via pathways like MAPK/ERK or PI3K/AKT and resistance to therapy. The crystallized structure enables structure-based design and molecular docking studies to identify potential inhibitors [9]. This research focuses on the design, synthesis, and bioactivity evaluation of 1,3,4-Oxadiazole derivatives as novel anti-HCC compounds. These derivatives show promise as anticancer agents due to their ability to target multiple pathways. The structural versatility of 1,3,4-Oxadiazole allows for further optimization, enhancing efficacy and minimizing potential side effects.

MATERIALS AND METHODS

Materials

All the required chemicals were procured from Lobachemie and Merck PVT LTD, Mumbai.

Method

Computational study

A virtual library comprising 30 newly designed 1,3,4-Oxadiazole ligands. The structure of derivative ligands is examined in Figure 1. These compounds feature a variety of functional groups with differing polarities, including amino, acetyl, methyl, hydroxyl, nitro, and halogen groups. The ligands were drawn using ChemDraw Ultra 2D 8.0 software, and Chem3D Ultra 8.0 software for molecular modeling, energy minimization using molecular mechanics, enabling calculation of molecular geometries, bond angles, and distances, and saved in .mol and .pdb formats for further computational studies [10].

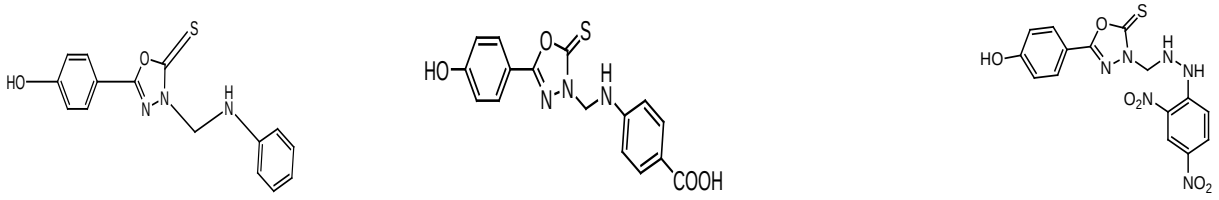

S1 **S9** **S23**

Figure 1: Structure of -1,3,4-Oxadiazole derivative (S1, S9, S23)

Early-stage in silico assessments were conducted to streamline compound selection, including Lipinski's Rule of Five**,** Molinspiration drug-likeness scores**,** and PreADMET predictions. These analyses suggested favorable pharmacokinetics and biological potential for the designed 1,3,4-Oxadiazole derivatives [11]. Molecular docking was carried out using Molegro Virtual Docker (MVD) with the MolDock SE algorithm (1500 iterations; population size: 50). The docking grid was centered on the active site of EGFR (PDB ID: 1M17)**,** targeting the co-crystallized ligand AQ4_999 within

a 15 Å radius cavity (volume: 270.848 Å³). Water molecules were excluded to ensure accurate binding predictions. Based on favorable docking scores and receptor interactions, 10 compounds were selected for further analysis [12]. The X-ray crystallographic structure of the PDB ID: 1M17, tyrosine EGFR kinaseenzyme, with the chemical name of [6,7-bis(2-methoxy-ethoxy)-quinazoline-4-yl]-(3-ethynylphenyl)amine, was retrieved from the RCSB. Reported amino acid interactions of PDB ID: 1M17 include the residues Met769 and Gln767, as well as neighboring residues Thr766, Lys721, Leu764, Asp831, Cys751, Lys828, Arg752, and Glu738 [13]. Docking scores were refined through MVD's internal energy minimization, accounting for hydrogen bonding**,** electrostatic**,** and steric interactions. 10 compounds with the most promising docking profiles were shortlisted for synthesis and biological evaluation.

Validation of Docking Methodology

To validate the protocol, the native ligand was re-docked into EGFR's active site. An RMSD < 2.0 Å between the docked and crystallographic pose confirmed the reliability of the docking setup [14].

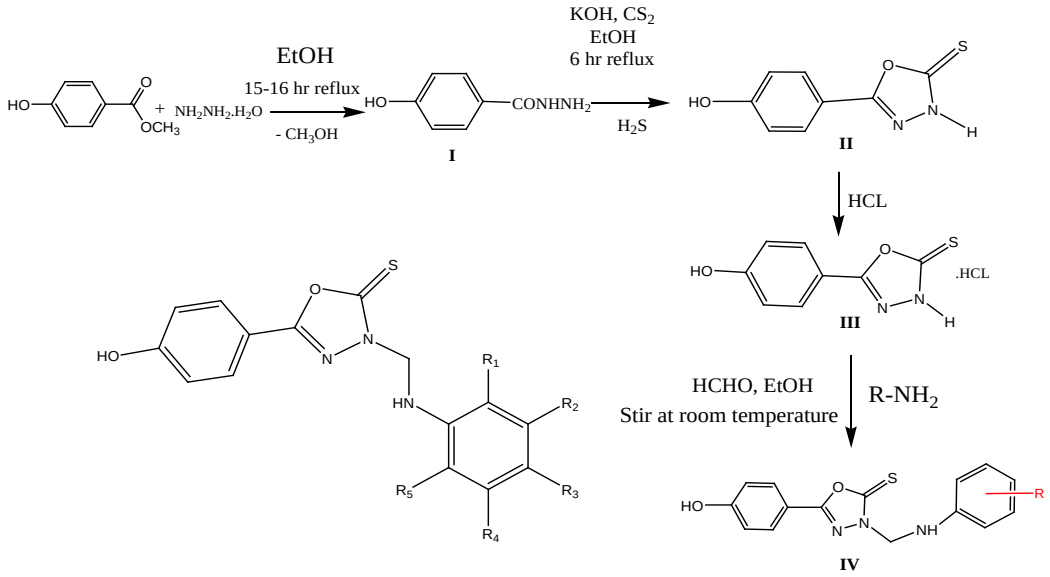

Figure 2: Synthesis Scheme of 1,3,4-Oxadiazole derivatives

SYNTHESIS OF DESIGNED COMPOUNDS

STEP 1: Synthesis procedure for Methyl 4-hydroxybenzoate derivatives

As the starting material, methyl 4-hydroxybenzoate (0.05 mol) was dissolved in 20 mL of ethanol, and 6.6 mL of hydrazine hydrate was added. The contents of the flask were then refluxed at 70°C for 15-16 hours. Upon completion of the reaction, the mixture was concentrated. To obtain the hydrazide derivatives (4-hydroxybenzo hydrazide), the reaction mixture was cooled with ice, filtered, washed, and dried. Then, the product was recrystallised with ethanol and dried.

STEP 2: Synthesis procedure for 4-hydroxybenzohydrazide derivatives

A mixture of 1 g (0.083 mol) of 4-hydroxybenzohydrazide and 0.56 g of potassium hydroxide was dissolved in 25 mL of ethanol at 25°C, and then 5 mL of carbon disulfide was gradually added. The mixture was continuously stirred for 6 hours. The derivative precipitated out, and the crude product was filtered and recrystallized from ethanol, followed by acidification with diluted HCl.

STEP 3: General procedure of 5-(4-hydroxyphenyl)-1,3,4-Oxadiazole-2(3H)-thione derivatives

The equimolar weight of intermediate 2(0.01 mol) was dissolved in 10 mL of ethanol and formaldehyde 40% (0.736 mL, 0.02 mol). Then, the appropriate amine (0.01 mol) was added and stirred at room temperature for 6-8 hours. After filtering and washing with cold ethanol, the precipitate was dried and recrystallised from ethanol (Figure 2 [15-20].

Spectral analysis of synthesis derivatives

The spectral analysis of the synthesized 1,3,4-Oxadiazole derivatives was recorded using a UV-Visible spectrophotometer

(Shimadzu Model 1800), an FT-IR spectrophotometer (Shimadzu 8400S), an NMR spectrophotometer (Bruker Advance Neo 500 MHz), and a GC Single Quad high-resolution mass spectrometer on the GC-MS (Agilent 7890A) instrument, respectively [20-24].

In-Vitro Biological Evaluation Procedure for SRB Assay (Sulphorhodamine-B Assay)

The HepG2 cell line is one of the most widely used in vitro models for HCC research. It retains many hepatic functions, such as albumin production, alpha-fetoprotein (AFP) expression, cytochrome P450 enzyme activity, lipid and glucose metabolism pathways. It is a commonly used HCC cell line that retains hepatic features and shows moderate EGFR expression, making it a suitable model for studying EGFR-targeted therapies in HCC. For the in vitro study, the HepG2 cell line was obtained from the NCCS, Pune, India. The cell lines were grown in appropriate medium containing 10% fetal bovine serum and 2 mM L-glutamine. Experiments were conducted using cells between passages 10 and 20 to ensure consistent growth characteristics. The Cell density is measured using the sulforhodamine B (SRB) assay, which quantifies cellular protein content. The refined technique enables 96-well toxicity screening of chemicals in adherent cell cultures. After incubation, cell monolayers are fixed with 10% (w/v) trichloroacetic acid, stained for 30 minutes, and repeatedly washed with 1% (v/v) acetic acid to eliminate any residual stain. The protein-bound dye is dissolved in a 10 mM Tris base solution, and the absorbance is read on an ELISA plate reader at 540 nm, with a reference wavelength of 690 nm. Adriamycin is used as a positive control, and untreated cells are used as a negative control. The method offers sensitivity similar to fluorometric techniques and provides linear results over a 20-fold range of cell counts. This method utilizes simple equipment and low-cost reagents, allowing for the rapid assessment of numerous samples within a short timeframe. As a result, the SRB assay is a very successful and economical screening technique [25-30].

Tyrosine Kinase Enzyme Inhibition Assay

Tyrosine kinases are a class of enzymes that selectively phosphorylate tyrosine substrates when a ligand is bound to the appropriate extracellular domain of the enzyme. Numerous signaling molecules, including EGFR, FGFR, PDGFR, VEGFR, and HGFR, are present in this extracellular region. The recombinant tyrosine kinase enzyme was purchased for the enzyme inhibition assay from Sigma-Aldrich, Mumbai.

Procedure: In DMEM media with 10% FCS, 4000-5000 HUVEC cells were seeded per well for the cell-based ELISA. The cells were serum-starved for 24 hours after incubation. Serum and test samples were administered, and the cells were then incubated at 37°C for 30 minutes. Once the media was removed, the cells were fixed using 4% formaldehyde in PBS.PBS was used 3 times to wash the cells. The cells were incubated for 1 hour with a 1:1000 anti-phospho EGFR (Tyr1092) antibody. After three washes with PBS-T, the cells were treated with an HRP-labeled secondary antibody (1:5000) for 1 hour. After washing, TMB was added to the cells. The reaction was halted with 2N H_2SO_4 and examined at 405 nm. Normalizing with the control determined the percentage inhibition [30-32].

Table 1: Results of Molinspiration and PreADMET study

Results of Molinspiration properties									
Code	**Properties**								
	mi LogP	**TPSA**	**n Atoms**	**MW**	**n OH**	**n OHNH**	**n Violations**	**n Rotb**	**Volume**
S1	2.65	63.22	21	299.36	5	2	0	4	254.72
S9	2.57	100.5	24	343.36	7	3	0	5	281.72
S23	2.26	106.9	28	404.36	9	3	0	7	213.79

Result of Biological activity						
Code	**GPCR ligand**	**Ion channel modulator**	**Kinase inhibitor**	**Nuclear receptor ligand**	**Protease inhibitor**	**Enzyme inhibitor**
S1	-0.81	-0.77	0.73	-0.85	-1.04	-0.04
S9	-0.67	-0.71	0.67	-0.56	-0.82	-0.02
S23	-0.70	-0.87	0.72	-1.08	-0.88	-0.19

Result of Drug Likeness of synthesized compounds		
Drug Likeness		**Compounds**
CMC_like_Rule	Qualified	S1, S9, S23
	Not qualified	-
MDDR_like_ Rule	Mid Structure	-
	Drug Like	S1, S9, S23
Rule_of_Five	Suitable	S1, S9, S23
	Not Suitable	-

Result of ADME properties					
Properties	**Range**	**Features**	**S1**	**S9**	**S23**
BBB(Blood Brain Barrier)	More than 1	CNS active compounds	1.382	-	-
	Less than 1	CNS inactive compounds	-	0.82	0.98
HIA (Human Intestinal Absorption)	0-20%	Poor absorption	-	-	-
	20-70%	Moderate absorption	-	-	67.59
	70-100%	Higher absorption	87.41	78.23	-
PPB (Plasma Protein Binding)	More than 90%	Strongly bounded	92.78	98.45	-
	Less than 90%	Weakly bounded	-	-	74.67
Caco-2 Permeability	Less than 4	Lower	-	-	-
	4-70	Moderate	21.58	20.47	19.24
	More than 70	Higher	-	-	-
CYP2D6	Non-inhibitor	Acceptance Yes	Non	Non	Non
	Inhibitor	Acceptance No	-	-	-
MDCK (Madin-Darby Canine Kidney)	Less than 25	Lower	10.23	8.97	3.48
	25-500	Moderate	-	-	-
	More than 500	Higher	-	-	-
P-gp_ Inhibition	Non-inhibitor	Acceptance No			
	Inhibitor	Acceptance Yes	Yes	Yes	Yes

Result of Toxicity studies		
Toxicity		**Compounds**
Ames_test	Mutagen	-
	Non-Mutagen	S1, S9, S23
Carcino_Mouse	Negative	S1, S9, S23
	Positive	-
Carcino_Rat	Negative	S1, S9, S23
	Positive	-
hERG_inhibition	Ambiguous	-
	Medium Risk	S1, S9
	Low-risk	S23

RESULTS

Result of Molecular Docking

The target compound exhibited strong activity, supported by high docking scores and favorable binding patterns, indicating its ability to interact with key amino acids in the EGFR binding site. The lead compounds S1, S9, and S23 demonstrated superior EGFR binding with initial MolDock scores of –117.78, –117.55, and –148.27 kcal/mol and refined re-rank scores of –91.60, –91.21, and –117.52 kcal/mol. These scores exceeded those of the co-crystallized ligand, which had docking scores of -124.917

and re-rank scores of -93.688 kcal/mol. Compound S23 demonstrated 4 significant hydrogen bonding interactions Met769, Gln767, Thr766, Asp831, and steric interaction of Glu738, Phe832, Asp831, Thr830 which is notably superior compared to standard drug Sorafenib, which exhibited only one hydrogen bond Lys721, Gly772 and steric interaction of Glu738, Thr830, Ala719, Pro770, Met 769, Cys773 with a docking score and re-rank score of -121.256 and -95.887 respectively.

Initial scores gauge basic ligand–receptor fit. In contrast, re-rank scores incorporate hydrogen bonds, van der Waals, ligand strain, and solvation for a more accurate prediction of binding stability and better differentiation between closely scoring ligands. The validation study's RMSD value for the dock orientation was found to be 1.78, which is lower than the crystal resolution of the 1M17 protein structure (2.60A0) reported in the protein data bank.

The molecular docking results, shown in Figure 3 and Table 2, suggest that these newly designed compounds could serve as potent EGFR inhibitors for anti-HCC.

STRUCTURAL ANALYSIS OF THE COMPOUNDS

3-((phenylamino)methyl)-5-(4-hydroxyphenyl)-1,3,4-Oxadiazole-2(3H)-thione(S1)

Yield: 68.63%, m.p. 178-180ºC, Rf = 0.66, UV (λ_{max}) nm = 299.34,(FTIR (CHCl3, υ/(cm-1): Aromatic C-H str (2998 cm^{-1}), C=N str (1634 cm^{-1}), C=S str (1028 cm^{-1}), O-H str (3367 cm^{-1}), Aromatic C=C str (1576 cm^{-1}), Aromatic C-H bnd (1384 cm^{-1}), C-H Bnd (1467 cm^{-1}), C-N str (1247 cm^{-1})**,** 1H NMR (500 MHz, CHCl3) δ (ppm): 6.26-7.87 (Ar H), 5.1 (Ar OH), 4.2 (aromatic C-NH), 4.56 (CH_2), 13C NMR (500 MHz, CHCl3) δ (ppm): 160.8 (C-OH), 177.6(N-C=S), 113.29-143.36 (Ar-C), 155.7 (N=C-O),68.4 (CH_2), ESI Mass *(m/z*, %): 299 (M+), 93: Hydroxyphenyl ion ($C_6H_4OH^+$) (100).

Figure 3: Docking Interactions of derivatives, Co-crystallized ligand and standard drug Sorafenib on PDB 1M17

S1	S9	S23
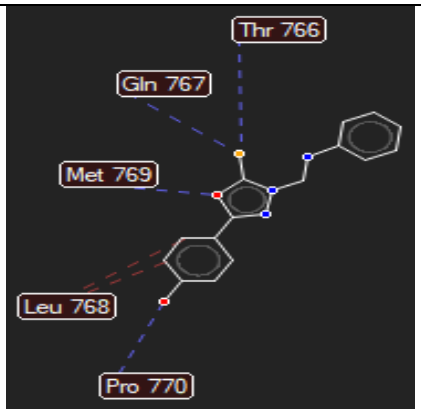	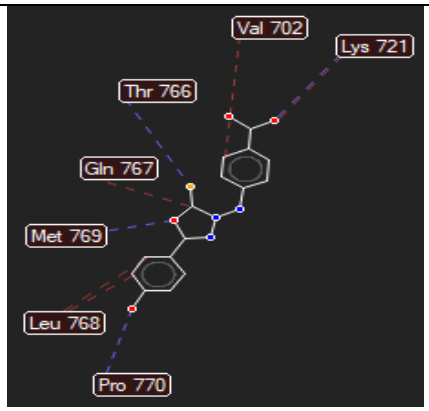	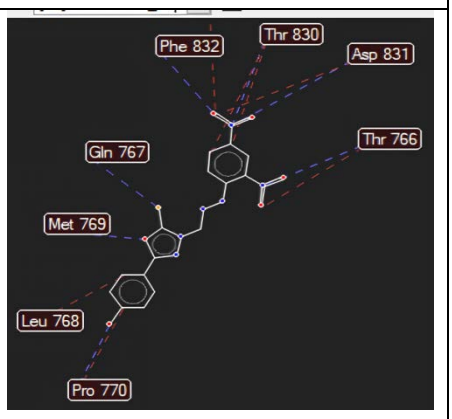
Docking View of Compound S23	**Docking Interaction of Co-crystallized ligand**	**Sorafenib**
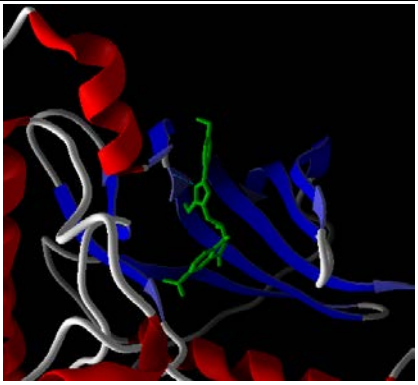	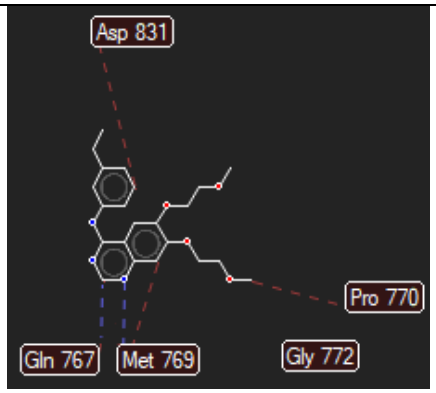	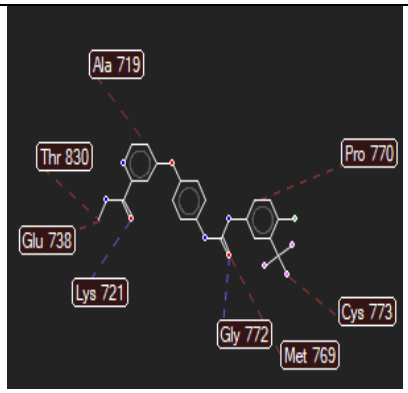
Docking View of Compound S23	**Docking Interaction of Co-crystallized ligand**	**Sorafenib**

Table 2: Docking score and interaction of 1,3,4-Oxadiazole derivatives

S No.	Comp.	Docking Score (Kj/mol)			Docking Interaction	
		Mol dock score	Rerank score	H-Bond	H-Bond interactions	Other Interaction
1.	S1	-117.78	-91.600	-7.229	Met 769, Gln767, Thr766	-------
2.	S3	-117.756	-84.884	-6.7136	Met 769, Gln767, Thr766	Leu764
3.	S9	-117.554	-91.207	-5.2367	Met 769, Gln767, Thr766	---------
4.	S10	-127.637	-98.405	-11.48	Met 769, Gln767, Thr766, Lus721	Leu764
5.	S11	-121.686	-91.630	-10.256	Met 769, Gln767, Thr766, Glu738	Leu764
6.	S15	-119.082	-81.826	-6.843	Met 769, Gln767, Thr766	Met769,Lys721,Leu764
7.	S18	-115.508	-88.202	-8.8763	Met 769, Gln767, Thr766	Leu764
8.	S23	-148.271	-117.52	-11.551	Met 769, Gln767, Thr766, Asp831	-------
9.	S27	-110.52	-87.282	-5.2927	Met 769, Gln767, Thr766, Glu738	Leu764
10.	S28	-104.089	-73.112	-9.5491	Met769, Thr766, Gln767	Lys721. Gln767
11.	Co-crystal	-124.917	-93.688	-1.9223	Met 769, Gln767	----------
12.	Sorafenib	-121.256	-95.887	-2.2489	Lys721, Gly772	Thr766

3-((4-nitrophenylamino)methyl)-5-(4-hydroxyphenyl)-1,3,4-Oxadiazole-2(3H)-thione (S3)

Yield: 73.15%, m.p. 155-157ºC, Rf = 0.71, UV (λ_{max}) nm =211.10, FTIR (CHCl3, υ/(cm-1): NO_2 -asymmetric str (1543 cm^{-1})**,** Nitro group symmetric str 1354, Aromatic C-H str (3023cm^{-1}), C=N str (1626 cm^{-1}), C=S str (967 cm^{-1}),O-H str (3268 cm^{-1}), Aromatic C=C str (1582 cm^{-1}), Aromatic C-H bnd (1402 cm^{-1}), C-H Bnd (1456 cm^{-1}), C--N str (1295 cm^{-1})**,** **1**H NMR (500 MHz, CHCl3) δ (ppm): 6.43 – 7.78 (Ar-H), 5.1 (Ar-OH), 4 (aromatic C-NH), 13C NMR (500 MHz, CHCl3) δ (ppm): 160.5 (C-OH), 176.3(N-C=S), 68.3 (CH_2), 155.6 (N=C-O), 114-145 (Ar-C), ESI Mass *(m/z*, %): 344 (M+), 93: Hydroxyphenyl ion ($C_6H_4OH^+$) (100).

4-((5-(4-hydroxyphenyl)-2-thioxo-1,3,4-Oxadiazol-3(2H)-yl)methylamino)benzoic acid (S9)

Yield: 79.24%, m.p. 204-206ºC, Rf = 0.84, UV (λ_{max}) nm = 262.30, FTIR (CHCl3, υ/(cm-1): Amide C=O str (1662 cm^{-1}), Carboxyl O-H str (2786 cm^{-1})**,** Aromatic C-H str (2964 cm^{-1}), C=N str (1642 cm^{-1}), C=S str (929 cm^{-1}),O-H str (3478 cm^{-1}), Aromatic C=C str (1553 cm^{-1}), Aromatic C-H bnd (1384 cm^{-1}), C-H bnd (1466 cm^{-1})**,** C--N str (1304 cm^{-1})**,**1H NMR (500 MHz, CHCl3) δ (ppm): 6.64-6.92 (Ar-H), 5.1 (Ar-OH), 4 (aromatic C-NH), 11.2 c of aromatic C-OH, 13C NMR (500 MHz, CHCl3) δ (ppm): 160.5 and 169.66 (C-OH), 178.3(N-C=S),67.9 (CH_2), 154.6 (N=C-O), 113-149 (Ar-C), ESI Mass *(m/z*, %): 343 (M+), 93: Hydroxyphenyl ion ($C_6H_4OH^+$) (100).

3-((2-hydroxyphenylamino)methyl)-5-(4-hydroxyphenyl)-1,3,4-Oxadiazole-2(3H)-thione (S10)

Yield: 73.82%, m.p. 190-192ºC, Rf = 0.77, UV (λ_{max}) nm =239.90, FTIR (CHCl3, υ/(cm-1): Aromatic C-H out-of-plane bnd (778 cm^{-1})**,** Aromatic C-H str (3029 cm^{-1}), C=N str (1653 cm^{-1}), C=S str (956 cm^{-1}),O-H str (3468 cm^{-1}), Aromatic C=C str (1579 cm^{-1}), Aromatic C-H bnd (1437 cm^{-1}), C-H Bnd (1472 cm^{-1}), C-N str (1247 cm^{-1})**,** 1H NMR (500 MHz, CHCl3) δ (ppm): 6.26-7.65 (Ar-H),4.42 (CH_2),5.11 Aromatic –OH, 4.15 (Ar-NH),13C NMR (500 MHz, CHCl3) δ (ppm): 160.78 and 141.6 (C-OH), 177.13(N-C=S), 67.5 (CH_2), 154.6 (N=C-O), 113-143 (Ar-C), ESI Mass *(m/z*, %): 315(M+), 93: Hydroxyphenyl ion ($C_6H_4OH^+$) (100).

3-((4-hydroxyphenylamino)methyl)-5-(4-hydroxyphenyl)-1,3,4-Oxadiazole-2(3H)-thione (S11)

Yield: 69.74%, m.p. 233-235ºC, Rf = 0.73, UV (λ_{max}) nm = 222.80, FTIR (CHCl3, υ/(cm-1): Aromatic C-H out-of-plane bnd (781 cm^{-1})**,**Aromatic C-H out-of-plane bnd (778 cm^{-1})**,** Aromatic C-H str (2967 cm^{-1}), C=N str (1648 cm^{-1}), C=S str (987 cm^{-1}),O-H str (3423 cm^{-1}), Aromatic C=C str (1576 cm^{-1}), Aromatic C-H bnd (1383 cm^{-1}), C-H Bnd (1464 cm^{-1}), C-N str (1341 cm^{-1})**,**1H NMR (500 MHz, CHCl3) δ (ppm): 6.26-7.54(Ar-H),4.42 methylene hydrogen,5.0 Aromatic –OH, 4.11 (Ar-NH), 13C NMR (500 MHz, CHCl3) δ (ppm): 160.78 and 146.9 (C-OH), 176.43(N-C=S), 67.5 (CH_2), 157.6 (N=C-O), 113.09-144.77 (Ar-C), ESI Mass *(m/z*, %): 315(M+), 93: Hydroxyphenyl ion ($C_6H_4OH^+$) (100).

N-((5-(4-hydroxyphenyl)-2-thioxo-1,3,4-Oxadiazol-3(2H)-yl)methyl)-N-phenylacetamide (S15)

Yield: 70.55%, m.p. 197-199ºC, Rf = 0.81, UV (λ_{max}) nm = 261.50, FTIR (CHCl3, υ/(cm-1): Amide C=O str (1678 cm^{-1})**,** Amide N-H bnd (1632 cm^{-1})**,** Aromatic C-H out-of-plane bnd (769 cm^{-1}), Aromatic C-H out-of-plane bnd (778 cm^{-1})**,** Aromatic C-H str (3039 cm^{-1}), C=N str (1608cm^{-1}), C=S str (1010 cm^{-1})**,** O-H str (3386 cm^{-1}), Aromatic C=C str (1559 cm^{-1}), Aromatic C-H bnd (1424 cm^{-1}), C-H Bnd (1474 cm^{-1}), C-N str (1269 cm^{-1})**,** 1H NMR (500 MHz, CHCl3) δ (ppm): 6.83-7.54 (Ar-H),5.2 (Ar-OH), 2.02 (CH_3),4.72 (-CH_2), 13C NMR (500 MHz, CHCl3) δ (ppm): 121.6 (Carbonyl carbon), 116.12-130.57 (Ar-C),66.3 (CH_2), 160.9 (C-OH), 177.73(N-C=S),155.6 (N=C-O), ESI Mass *(m/z,* %): 340(M+), 93: Hydroxyphenyl ion ($C_6H_4OH^+$) (100).

5-(4-hydroyphenyl)-3-((pyridine-2-ylamino)methyl)-1,3,4-Oxadiazole-2(3H)-thione (S18)

Yield: 75.68%, m.p. 215-217ºC, Rf = 0.76, UV (λ_{max}) nm = 243.20,FTIR (CHCl3, υ/(cm-1): Pyridine C-H bnd (1393 cm^{-1}), Aromatic C-H out-of-plane bnd (787 cm^{-1})**,** Aromatic C-H str (2986 cm^{-1}), C=N str (1603 cm^{-1}), C=S str (976 cm^{-1}), O-H str (3453 cm^{-1}), Aromatic C=C str (1575 cm^{-1}), Aromatic C-H bnd (1385 cm^{-1}), C-H Bnd (1464 cm^{-1}), C-N str (1326 cm^{-1})**,** 1H NMR (500 MHz, CHCl3) δ (ppm): 6.45-8.41 (Ar-H),5.23 (Ar-OH), 4.42 (-CH_2), 4.32 (Ar-NH), 13C NMR (500 MHz, CHCl3) δ (ppm): 109.22-158.51 (Ar-C),66.7 (CH_2), 161.1 (C-OH), 176.73(N-C=S), 157.1 (N=C-O), ESI Mass *(m/z,* %): 300 (M+), 93: Hydroxyphenyl ion ($C_6H_4OH^+$) (100).

3-{[2-(2,4-dinitrophenyl)hydrazinyl]methyl}-5-(4-hydroxyphenyl)-1,3,4-Oxadiazol-2(3H)-thion (S23)

Yield: 72.84%, m.p. 119-121ºC, Rf = 0.63, UV (λ_{max}) nm = 232.40, FTIR (CHCl3, υ/(cm-1): NO_2 -asymmetric str (1544 cm^{-1})**,** NO_2- symmetric str (1349cm^{-1})**,** Aromatic C-H str (3038 cm^{-1}), C=N str (1639 cm^{-1}), C=S str (1041 cm^{-1}), O-H str (3305 cm^{-1}), Aromatic C=C str (1528 cm^{-1}), Aromatic C-H bnd (1364 cm^{-1}), C-H Bnd (1473 cm^{-1}), C-N str (1326 cm^{-1})**,** 1H NMR (500 MHz, CHCl3) δ (ppm): 6.76-9.44 (Ar-H),5.18 (Ar-OH), 4.12 (Ar-NH), 13C NMR (500 MHz, CHCl3) δ (ppm): 115.45-135.65 (Ar-C),68.7 (CH_2), 160.3 (C-OH), 176.03(N-C=S), 156.1 (N=C-O), ESI Mass *(m/z,* %): 404(M+), 93: Hydroxyphenyl ion ($C_6H_4OH^+$) (100).

4-({[5-(4-hydroxyphenyl)-2-sulfanylidene]-1,3,4-Oxadiazol-3(2H)-yl)methyl}amino)benzene-1-sulfonamide (S27)

Yield: 76.86%, m.p. 240-242ºC, Rf = 0.65, UV (λ_{max}) nm = 274.60, FTIR (CHCl3, υ/(cm-1**):** Sulfonamide S=O str (1276 cm^{-1})**,** Aromatic C-H out-of-plane bnd (793 cm^{-1}), Aromatic C-H str (2943 cm^{-1}), C=N str (1647 cm^{-1}), C=S str (966 cm^{-1}), O-H str (3497 cm^{-1}), Aromatic C=C str (1579 cm^{-1}), Aromatic C-H bnd (1393 cm^{-1}), C-H Bnd (1469 cm^{-1}), C-N str (1276 cm^{-1})**,** 1H NMR (500 MHz, CHCl3) δ (ppm): 6.68-7.56 (Ar-H),5.0 (Ar-OH), 4 (Ar-NH), 2.12 (Amine), 13C NMR (500 MHz, CHCl3) δ (ppm): 116.55-134.68 (Ar-C), 69.3(CH_2), 159.8 (C-OH), 176.93(N-C=S), 155.1 (N=C-O), ESI Mass *(m/z,* %): 378 (M+), 93: Hydroxyphenyl ion ($C_6H_4OH^+$) (100).

1-((5-(4-hydroxyphenyl)-2-thioxo-1,3,4-Oxadiazol-3(2H)-ylmethyl)urea (S28)

Yield: 84.65%, m.p. 265-257ºC, Rf = 0.77, UV (λ_{max}) nm = 245.60, FTIR (CHCl3, υ/(cm-1): Amide N-H bnd (1639 cm^{-1})**,** Aromatic C-H out-of-plane bnd (784 cm^{-1}), Aromatic C-H str (2969 cm^{-1}), C=N str (1632 cm^{-1}), C=S str (1042 cm^{-1}), O-H str (3385 cm^{-1}), Aromatic C=C str (1586 cm^{-1}), Aromatic C-H bnd (1431 cm^{-1}), C-H Bnd (1477 cm^{-1}), C-N str (1330 cm^{-1})**,**1H NMR (500 MHz, CHCl3) δ (ppm): 6.76-7.83 (Ar-H),5.0 (Ar-OH), 4.52 (CH_2),6.02 (Amine), 13C NMR (500 MHz, CHCl3) δ (ppm): 162.45 (Carbonyl carbon), 61.6 (CH_2), 114.57-132.45 (Ar-C), 178.13(N-C=S), 156.06 (N=C-O), ESI Mass *(m/z,* %): 266 (M+), 93: Hydroxyphenyl ion ($C_6H_4OH^+$) (100).

Result of In-Vitro Evaluation Procedure for SRB Assay (Sulphorhodamine-B Assay)

The results of in vitro testing for the presence of anticancer activity on the Hep-G2 cell line revealed that both electron-releasing groups (-H) and electron-withdrawing groups (-COOH, -NO_2) significantly boost the anticancer activity against the hepatoma cell line. Out of all the synthetic derivatives, compounds S1, S9, and S23 show good to moderate cytostatic activity at 10^{-4}M concentration doses. The substitution pattern significantly impacts the biological activity on the oxadiazole ring. The GI_{50} for three, S1, S9, and S23 (images are displayed in the figure), were 0.486, 0.334 & 0.256, respectively. Anticancer activity results indicate that substitution at positions ortho and para on the phenyl ring significantly boosts activity. The result is shown in Table 3 and Figure 4, the comparative growth inhibitory activity of all synthetic compounds in comparison to the reference standard drug (Adriamycin).

Table 3: Percentage control growth and growth inhibition (GI50) value of human hepatoma cell line Hep-G2

Comp. Code	% Control Growth (Mean ± SEM, N=3) Molar Drug Concentrations				Growth Inhibition GI_{50} in (µM) Conc.
	10^{-7}M	10^{-6}M	10^{-5}M	10^{-4}M	
S1	116.6	125.7	128.8	46.7	0.48677555
S3	118.3	125.2	139.4	110.8	0.00033198
S9	112.7	122.8	147.3	37.6	0.33446465
S10	111.2	121.9	146.0	123.5	0.00006428
S11	109.0	129.8	144.6	120.7	0.00043459
S15	118.9	131.9	142.0	114.0	0.00001459
S18	109.9	128.3	136.2	79.8	0.00004284
S23	129.1	133.2	141.4	28.4	0.25665634
S27	130.8	128.9	146.7	118.0	0.00001119
S28	129.5	135.3	141.5	119.0	0.00020286
ADR	17.6	-13.7	-21.2	-38.7	8.10000000

Result of Tyrosine Kinase Enzyme Inhibition Assay

Upon cellular screening on Hep-G2 cell line, compound S23 emerges as a good anticancer agent. To investigate the mode of action of the synthesized compound, it was subjected to an enzyme inhibition assay. Kinase inhibitory activity of compound S23 was screened using an ELISA procedure and compared with that of Staurosporine as a reference drug. S23 exhibits good inhibitory activity with an IC50 value of 1.87µg/ml Table 4 and Figure 5. The activity of this compound is due to the electron-withdrawing group (-NO_2 at the para and ortho positions. As reported in the literature, the surface of the tyrosine kinase is mainly hydrophobic. Electron-withdrawing groups can alter the electron density of adjacent aromatic rings or other groups, enabling stronger π-π stacking with aromatic residues in the tyrosine kinase binding pocket and exhibiting significant inhibitory activity, which suggests that our synthesized compound might be a good inhibitor of tyrosine kinase enzyme.

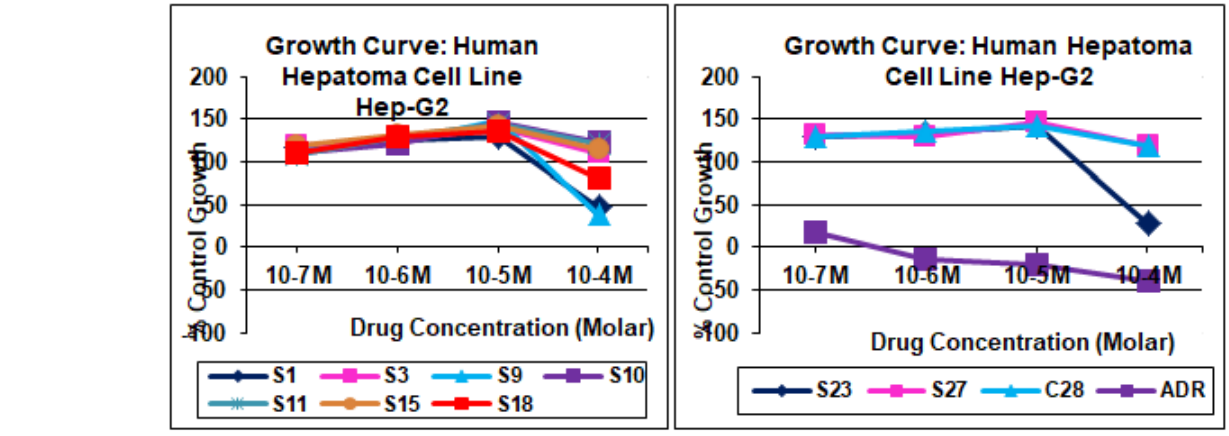

a

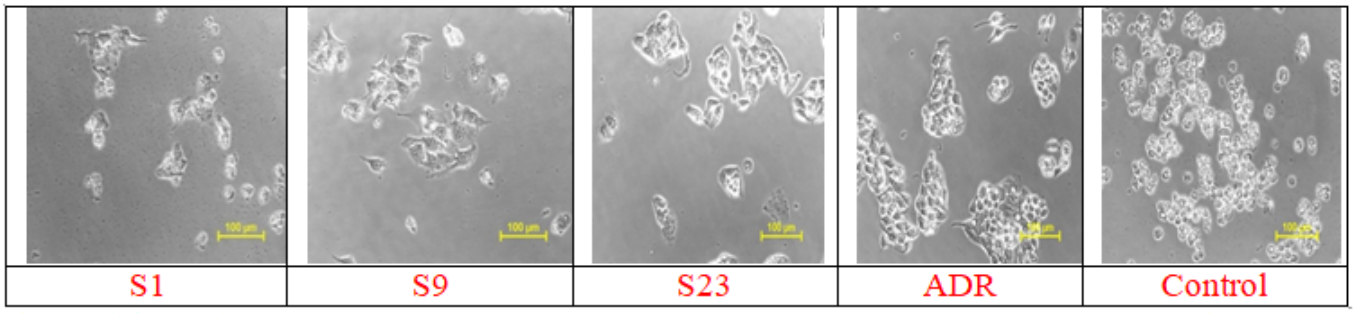

b

Figure 4: (a) Growth curve of Hep-G2Cell line, (b) Images of In-vitro screening of synthesized derivatives S1, S9, and S23 of 1,3,4- Oxadiazole derivative for anticancer activity on Hep-G2 cell line

DISCUSSION

The 1,3,4-Oxadiazole derivatives follow Lipinski's rule, indicating drug-likeness, and PreADMET analysis shows high bioavailability with low toxicity. S1, S9, and S23 demonstrate strong EGFR inhibition in docking studies. S23 outperforms Sorafenib with superior binding interactions. The *in silico* results align with known experimental data on EGFR inhibitors, showing similar binding affinities and key interactions, such as

Met769, Gln767, Thr766, and Asp831. S23 exhibited a strong affinity comparable to Sorafenib in docking studies, which is supported by experimental data of IC50 and GI50 values **Table 5**. However, S23 also displayed unique features, such as a highly lipophilic, low toxicity profile and high yield value, which may offer advantages over current therapies. These differences warrant further experimental validation to confirm their potential in EGFR-targeted cancer treatment.

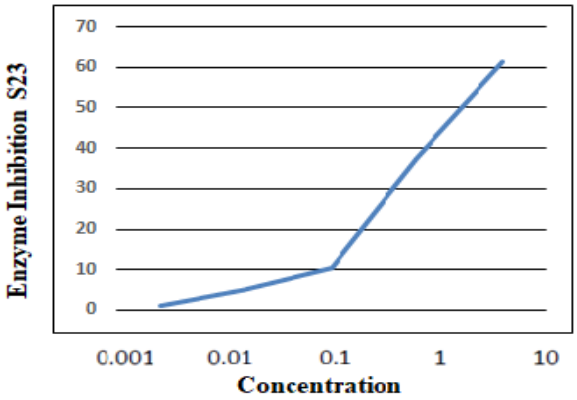

Figure 5: % enzyme inhibition of synthesized compound S23

Table 4: % enzyme inhibition of synthesized compound S23

Concentration	S23
10	61.32
1	37.26
0.1	10.52
0.01	5.25
0.001	1.02
IC_{50}VALUE µM	1.87
StaurosporineIC_{50}	0.1

These compounds are promising candidates for targeted cancer therapy. The FTIR spectra showed characteristic stretching vibrations, confirming the presence of key bonds like C=O, N-H, and C-N.^{1}H NMR analysis revealed chemical shifts corresponding to aromatic and aliphatic protons, supporting the proposed structure.^{13}C NMR analysis confirmed the placement of carbon atoms in the structure, validating the compound's framework. Mass spectrometry analysis showed molecular ion peaks consistent with the expected molecular weights of the compounds. In-vitro testing of Compounds S1, S9, and S23 exhibited good to moderate cytostatic activity at a concentration of 10^{-4} M. Substitution at ortho and para positions by electron-releasing (-H) and electron-withdrawing (-COOH, -NO2) groups enhances cytotoxic potential toward Hep-G2 cells. The Tyrosine Kinase Enzyme Inhibition Assay was conducted to evaluate the effectiveness of potential inhibitors in disrupting tyrosine kinases' phosphorylation activity. These enzymes regulate vital cellular functions and are critically involved in the pathogenesis of cancer. Together, these assays deliver a thorough insight into derivative molecules' biological effects and therapeutic potential.

Table 5: Correlation of docking scores and bioactivity data of derivatives

Compound Code	Docking Score (Kcal/mol)	Total No. of Interactions	GI_{50} (µM)
S1	-117.78	5	0.48677555
S9	-117.554	7	0.33446465
S23	-148.271	8	0.25665634

CONCLUSION

The 1,3,4-Oxadiazole derivatives evaluated in this study fulfill Lipinski's Rule of Five, indicating favorable pharmacokinetic profiles with good bioavailability and low toxicity. Among them, compounds S1, S9, and particularly S23 exhibited significant inhibition of EGFR, with S23 surpassing the standard drug Sorafenib in activity. The superior performance of S23 can be attributed to its unique functional groups and molecular geometry, which enhance its binding orientation and ability to form hydrogen bonds within the EGFR active site. Molecular docking studies confirmed strong binding affinities of the derivatives, especially S23, which showed key interactions with amino acid residues such as Lys721, Thr766, and Met769. These I*n-silico* results correlated well with the in vitro cytotoxicity assays, where compounds with better docking scores also demonstrated lower IC_{50}/GI_{50} values, supporting their biological activity. SAR analysis further revealed that aromatic amines and electron-withdrawing groups were critical in inhibiting tyrosine kinase. Spectroscopic techniques, including Mass, NMR, and FTIR, confirmed the key functional groups' structural integrity and presence. The compounds exhibited moderate cytostatic activity, with ortho and para substitutions enhancing anticancer effects. Additionally, tyrosine kinase inhibition assays confirmed the compounds' potential in modulating cancer-related signaling pathways.

Compound S23 emerged as the most promising lead, demonstrating high binding affinity, potent EGFR selectivity, and favorable pharmacokinetics. Modifications to its nitro group may further enhance efficacy and reduce off-target interactions. These findings highlight S23 and related 1,3,4-Oxadiazole

derivatives as strong candidates for further preclinical development in targeted cancer therapy, with molecular docking providing a reliable predictive framework for activity validation.

ACKNOWLEDGEMENTS
The authors would like to acknowledge the GRY Institute of Pharmacy, Borawan, for providing the research facilities, Deshpande Laboratories Pvt. Ltd. in Bhopal, Madhya Pradesh, for assessing the effectiveness of synthetic chemicals as tyrosine kinase inhibitors, ACTREC Tata Memorial Centre, Navi Mumbai, Mass, and NMR center instrument facility IISER Bhopal, for IR Indira Gandhi National Tribal University, Amarkantak, India.

CONFLICT OF INTEREST
The authors declare no conflict of interest.

FUNDING SOURCES
NIL

AUTHOR CONTRIBUTION
All authors have reviewed and approved the final version of the manuscript and accept collective responsibility for the entire work. Nitin Deshmukh conceived and designed the study. Mohini Patidar conducted data collection, analysis, interpretation, and original drafting. Raghvendra Dubey completed the final approval of all the work and the manuscript.

REFERENCES
[1] Marina GM, Jorge AS, et al. Liver Cancer: Therapeutic Challenges and the Importance of Experimental Models. *Canadian Journal of Gastroenterology and Hepatology*, **8837811**, 1-10 (2021) https://doi.org/10.1155/2021/8837811.

[2] Ma Y-S, Liu J-B, Wu T-M, Fu D. New Therapeutic Options for Advanced Hepatocellular Carcinoma. *Cancer Control*, **27**, 1-11 (2020) https://doi.org/10.1177/1073274820945975.

[3] Qiushi Y, Xiaolong H, et al. LncRNA model predicts liver cancer drug resistance and validate in vitro experiments. *Front. Cell Dev. Biol*, **11**, 1174183 (2023) https://doi.org/10.3389/fcell.2023.1174183.

[4] Faisal K, Chatterjee S, Bhojani G, Sen S, et al. Seaweed polysachharide derived Bioaldehyde nanocomposite: Potential application in anticancer therapeutics. *Carbohydrate Polymers*, **240**, 116282 (2020) https://doi.org/10.1016/j.carbpol.2020.116282.

[5] Yan J. New knowledge of the mechanisms of Sorafenib resistance in liver cancer. *Acta Pharmacologica Sinica*, **38**, 614–622 (2017) https://doi.org/10.1038/aps.2017.5.

[6] Rathod S. Recent court orders in patent suits on limits of Bolar exemption: Shrinking space for pharmaceutical generic companies in India?. *Journal of generic medicines*, **18(3)**, 1-10 (2021) https://doi.org/10.1177/17411343211038999.

[7] Zuhair A, Sarah AH, et al. Studying the anti-cancer activity of Resveratrol 1,3,4-Thiadiazol derivatives. *Research J. Pharm. and Tech.*, **15(10)**, 4377-1 (2022) https://doi.org/10.52711/0974-360X.2022.00734.

[8] Zahraa TK, Entesar OAT. Synthesis, Identification, Theoretical Study and effect of 1,3,4-Oxadiazole Compounds Substituted on Creatinine ring on the activity of some Transfers Enzymes. *Research J. Pharm. and Tech.*, **12(8)**, 3581-3588 (2019) https://doi.org/10.5958/0974-360X.2019.00611.5.

[9] Bang J, Jun M, Lee S, Moon H, Ro SW. Targeting EGFR/PI3K/AKT/mTOR signaling in hepatocellular carcinoma. *Pharmaceutics*, **15(8)**, 2130 (2023) https://doi.org/10.3390/pharmaceutics15082130.

[10] Pavlo VZ, Vadym VK, Teslenko N, et al. In Silico Prediction and Molecular Docking Studies of N-Amidoalkylated Derivatives of 1,3,4-Oxadiazole as COX-1 and COX-2 Potential Inhibitors. *Research J. Pharm. and Tech*., **10(11)**, 3957-3963 (2017) https://doi.org/10.5958/0974-360X.2017.00718.1.

[11] Stamos J, Sliwkowski M, Eigenbrot C. Structure of the Epidermal Growth Factor Receptor Kinase DomainAlone and in Complex with a 4-Anilinoquinazoline Inhibitor. *The journal of biological chemistry*, **277,** 46265–4272 (2002) https://doi.org/10.1074/jbc.M207135200.

[12] Bala S, Kamboj S, Anu K, Saini V, Deo N. 1,3,4-Oxadiazole Derivatives: Synthesis, Characterization, Antimicrobial Potential, and Computational Studies. *Biomed Res Int.*, **172791,** 18(2014) https://doi.org/10.1155/2014/172791

[13] Singhai A, Gupta MK. Synthesis and Characterization of 1,3,4-Oxadiazole Derivatives as Potential Anti-inflammatory and Analgesic agents. *Research J. Pharm. and Tech.*,**13(12),** 5898-5902 (2020) https://doi.org/10.5958/0974-360X.2020.01029.X.

[14] Pavlo VZ, Ihor OP, Vadym VK, Oxana VO, Aleksandr VK. Molecular Docking Studies of N-(((5-Aryl-1,3,4-oxadiazol-2-yl)amino)methyl)- and N-(2,2,2-Trichloro-1-((5-aryl-1,3,4-oxadiazol-2-yl)amino)ethyl)carboxamides as Potential Inhibitors of GSK-3β. *Research J. Pharm. and Tech.*, **12(2),** 523-530 (2019) https://doi.org/10.5958/0974-360X.2019.00092.1.

[15] Camelia E. Synthesis and Anticancer Evaluation of New1,3,4-Oxadiazole Derivatives. *Pharmaceuticals*, **14**, 438 (2021) https://doi.org/10.3390/ph14050438.

[16] Ragab F, Abou-Seri S, Salah A, et al. Design, synthesis and anticancer activity of new monastrol analogues bearing 1,3,4-oxadiazole moiety. *European Journal of Medicinal Chemistry*, **17**, 30472-510 (2017) https://doi.org/1016/j.ejmech.2017.06.026.

[17] Bajaj S, Roy P, Singh J. Synthesis, Thymidine Phosphorylase inhibitory and computational study of novel 1,3,4-oxadiazole-2-

thionederivatives as potential anticancer agents. *Computational Biology and Chemistry*, **18**, 1-36 (2018) https://doi.org/10.1016/j.compbiolchem.2018.05.013.

[18] Chakrabhavi D. Noval 1,3,4-oxadiazole induce anticancer activity by targeting NF-kB in hepatocellular carcinoma cell, *Front. Oncol*, **8**, 42(2018) https://doi.org/10.3389/fonc.2018.00042.

[19] Stamos J, Sliwkowski M, Eigenbrot C. Structure of the Epidermal Growth Factor Receptor Kinase Domain Alone and in Complex with a 4-Anilinoquinazoline Inhibitor. *The journal of biological chemistry*, **277**, 46265–46272 (2002) https://doi.org/10.1074/jbc.M207135200.

[20] Puttaswamy N, Malojiao V, Yasser H, et al. Synthesis and amelioration of inflammatory paw edema by novel benzophenone appended oxadiazole derivatives by exhibiting cyclooxygenase-2 antagonist activity. *Biomedicine & Pharmacotherapy*, **103**, 1446–1455 (2018) https://doi.org/10.1016/j.biopha.2018.04.167.

[21] Yadav N, Kumar P, Chhikara A, Madhu, et al. Development of 1,3,4-oxadiazole thione based novel anticancer agents: Design, synthesis and in-vitro studies. *Biomedicine & Pharmacotherapy*, **95**, 721–730 (2017) http://dx.doi.org/10.1016/j.biopha.2017.08.110.

[22] Pidugu V, SastryYarla N, Pedada S, Kalle A, Satya K. Design and synthesis of novel HDAC8 inhibitory 2,5-disubstituted-1,3,4-oxadiazoles containing glycine and alanine hybrids with anticancer activity. *Bioorganic & Medicinal Chemistry*, **24**, 5611–5617 (2016) http://dx.doi.org/10.1016/j.bmc.2016.09.022.

[23] Kumar D, Sundaree S, Johnson EO, Shah K. An efficient synthesis and biological study of novel indolyl- 1, 3, 4-oxadiazoles as potent anticancer agents. *Bioorg. Med. Chem. Lett.*, **19 (15)**, 4492–4494 (2009) http://dx.doi.org/10.1016/j.bmcl.2009.03.172.

[24] Abdel-Aziz MA, Metwally K, Gamal-Eldeen AM, et al. 1,3,4-oxadiazole-2-thione derivatives; novel approach for anticancer and tubulin polymerization inhibitory activities. *Anti-Cancer Agents Med. Chem.*, **16(2),** 269–277 (2016) 10.2174/1871520615666150907093855.

[25] Vichai V and Kirtikara K. Sulforhodamine B colorimetric assay for cytotoxicity screening. *Nature Protocols*, **1(3)**, 1112-6 (2006) http://dx.doi.org/10.1038/nprot.2006.179.

[26] Kode J, Kovvuri J, Nagaraju B, et al. Synthesis, biological evaluation and molecular docking analysis of phenstatin based indole linked chalcones as anticancer agents and tubulin polymerization inhibitors. *Bioorganic Chemistry*, **105**, 104447 (2020) https://doi.org/10.1016/j.bioorg.2020.104447.

[27] Skehan P, Storeng R, Scudiero D, et al. New colorimetric cytotoxicity assay for anticancer-drug screening. *J Natl Cancer Inst.*, **82**, 1107-1112 (1990).

[28] Mosmann T. Rapid colorimetric assay for cellular growth and survival: application to proliferation and cytotoxicity assays. *J. Immunol. Methods*, **65 (1-2)**, 55–63(1983) 10.1016/0022-1759(83)90303-4.

[29] Ahmad A, Varshney H, Rauf A, A Sherwani, M Owais. Synthesis and anticancer activity of long chain substituted 1, 3, 4-oxadiazol-2-thione, 1, 2, 4-triazol-3-thione and 1, 2, 4-triazolo 3,4-b-1, 3, 4-thiadiazine derivatives. *Arab. J. Chem.*, **10 (2)**, S3347–S3357 (2017) https://doi.org/10.1016/j.arabjc.2014.01.015.

[30] Gudipati R, Anreddy RNR, Manda S. Synthesis, characterization and anticancer activity of certain 3-{4-(5-mercapto-1, 3, 4-oxadiazole-2-yl) phenylimino} indolin-2-one derivatives, *Saudi Pharm. J.*,**19 (3)**, 153–158 (2011) https://doi.org/10.1016/j.jsps.2011.03.002.

[31] Qinlian J, Lei Bi, Yidan R, Song S, et al. Advances in studies of tyrosine kinase inhibitors and their acquired resistance. *Molecular Cancer*, **17**, 36 (2018) https://doi.org/10.1186/s12943-018-0801-5.

[32] Labots M, Gotink K J, Dekker H, et al. Evaluation of a tyrosine kinase peptide microarray for tyrosine. kinase inhibitor therapy selection in cancer. *Experimental & Molecular Medicine*, **48**, 279 (2016) https://doi.org/10.1038/emm.2016.114.

[33] Josephine MA, Naichen Y, Xiaobo W, Xiao Xu, et al. Label-Free and Real-Time Cell-Based Kinase Assay for Screening Selective and Potent Receptor Tyrosine Kinase Inhibitors Using Microelectronic Sensor Array. *Journal of Biomolecular Screening*, **11(6)**, 10 (2006) https://doi.org/10.1177/1087057106289334.